Atom Indonesia

Journal homepage: http://aij.batan.go.id

Simulation of Leksell Gamma Knife-4C System with Different Phantoms Using PHITS and Geant4

B. T. Hung[1], T. T. Duong[2*], B. N. Ha[2]

[1]*Vietnam Atomic Energy Institute, No 59 Ly Thuong Kiet, Hanoi, Vietnam*
[2]*University of Science and Technology, No 1 Dai Co Viet, Hanoi, Vietnam*

ARTICLE INFO

Article history:
Received 18 August 2022
Received in revised form 20 September 2022
Accepted 28 September 2022

Keywords:
Leksell gamma knife
Reference computational phantoms
PHITS
Geant4

ABSTRACT

This study used PHITS and Geant4 code packages to simulate a Leksell Gamma Knife system in order to determine radiation dose distribution in two types of phantoms. The results observed in the water phantom with configurations of single source and 201 sources are in good accord with the prior research, including both simulation and experiment. Several characteristics of Leksell Gamma Knife 4C, such as dose profiles, output factor, FWHM, and penumbra size, are calculated based on Monte Carlo simulations, which show the best consistency with other results. The output factors for collimators of 14 mm, 8 mm, and 4 mm are 0.984, 0.949, and 0.872, respectively. The simulation results with an adult mesh-type reference phantom reveal considerable similarities with the established radiosurgery plans. It indicates that the absorbed dose in brain tumors was highest when utilizing the 18 mm collimator and subsequently reduced with collimator size to 0.65, 0.25, and 0.5 with the 14 mm, 8 mm, and 4 mm collimators, respectively. The absorbed dose has a very low value for other essential organs and decreases with distance from the brain tumor. These findings may explain why the dose to organs decreases linearly as target distance, volume, and collimator size increase.

INTRODUCTION

The term "radiosurgery" was first introduced by a Swedish neurosurgeon named Lars Leksell in 1958. This technique uses extremely narrow gamma beams emitted by isotope radiation sources focused on the target tissue to be destroyed through a collimator system while still ensuring the safety of surrounding healthy tissue. It is commonly used to kill tumors, particularly brain tumors. Today, stereotactic radiosurgery has become one of the essential tools for neurosurgeons [1]. It has replaced the methods of open surgery and laparoscopic surgery because these methods have the risk of leaving complications with damage to the brain or nervous system during the procedure. Radiosurgery provides the patient with the benefits of no discomfort, no sequelae, only one treatment, and the quickest recovery.

In the late 1960s, Larsson and Leksell designed the first device that used multiple cobalt sources. The first Gamma Knife was installed at Sophiahemmet in Stockholm in 1968. Up to now, the Gamma Knife radiosurgery system has been classified into two types based on the motion characteristics of the radioactive sources: stationary and rotating systems. The Model U, Model B, Model C, Model 4C, and Perfexion are designs of static device generations [1]. The source geometry and dimensions of Model U are identical to those of Models B and C, with the exception of a higher latitude angle [2]. Model C is similar to Model B but has an Automatic Positioning System (APS). APS was a feature of both the Model C and the Model 4C, but it has been replaced by the Patient Positioning System (PPS) in the Leksell Gamma Knife (LGK) Perfexion. Instead of just moving the patient's head, as in the APS system, the new system may move the patient's entire body based on pre-selected stereotactic coordinates. The rotating systems come in two varieties: Gamma ART-6000 (later renamed Vertex360 in 2008 [3]) and OUR. The common feature of both the two types is the use of high-intensity cobalt sources; the difference is the number of sources used, the state of motion, and the activity of each source.

*Corresponding author.
E-mail address: duongtran902@gmail.com
DOI:

In all radiotherapy and radiosurgery systems, as well as gamma knife systems, measuring and calculating dose distribution and other physical parameters play an extremely important role in ensuring the quality of the planning system. However, due to the inherent problems of physical dosimetry, the Monte Carlo (MC) simulation method has been used as a useful supplement to achieve the goal. Nowadays, the MC method has become an indispensable tool along with experiments to carry out dose calculation studies in the human body by using the built-in simulation code. Researchers can use virtual experiments for dose estimation and assessment in human organs, allowing them to analyze the absorbed dose and dose distribution, as well as evaluate the effect and provide recommendations [2,6-9]. Simulation code packages such as MCNP, PHITS, Geant4, EGS, FLUKA, PENELOPE, and others are commonly utilized for these purposes. To date, there have been several studies on calculating dose distribution in radiosurgery with the Leksell Gamma Knife systems [6-12]. These studies were carried out using both experimental and Monte Carlo simulation methods. However, they have only used spherical water phantoms to replace human subjects. As a result, it does not accurately reflect the physical effects that occur and may vary by patient. While such limitations still exist, we have conducted research by simulating a Leksell Gamma Knife system in order to determine the radiation dose distribution in two types of phantoms. This work has been accomplished via the PHITS code, which now includes numerous additional features for mesh and voxel geometries. Additionally, Geant4 was utilized to compare and evaluate the dependability of PHITS simulation calculations.

METHODOLOGY

In this study, the Leksell Gamma Knife Model 4C was modeled by using the PHITS code package. PHITS (Particle and Heavy Ion Transport code System) is a general-purpose Monte Carlo-based radiation transport code system developed through the collaboration of several institutes in Japan and Europe [3]. It can deal with the transport of nearly all particles, including neutrons, protons, heavy ions, photons, and electrons, over wide energy ranges using several nuclear reaction models and nuclear data libraries [4]. PHITS does not require the user to have programming skills because its input file is completely written in the same free text as MCNP. Three-dimensional geometry is supported with GG (General Geometry) format, which is a type of geometry that allows construction from basic blocks through associative operators. The study also used Geant4 version 10.07 to analyze the simulation results of PHITS for LGK. This is one of the most effective tools in Monte Carlo simulation. It is possible to simulate almost all the different types of particles over a wide energy range with the support of many physics libraries. Because it is built on object-oriented programming languages and techniques, Geant4 is very flexible. In particular, Geant4 provides a wide variety of tools and solutions for describing geometry setups, from simple to highly complex. Recent extensions of the geometry modeler include specialized navigation techniques and optimization algorithms to aid medical simulation research. It has allowed complex geometrical models of the human body to be developed [18].

The Leksell stereotactic gamma knife's main components are radiation sources with four types of collimator helmets, a patient treatment table, a hydraulic system, and a control panel [4]. This research concentrated on simulating the source unit and collimators, which have the same geometric structure as the work of Al-Dweri et al. [5]. Figure 1 shows the schematic view of the modeled geometry in the PHITS simulation. Figure 1(a) demonstrates the general structure of a source channel that includes three parts (source, primary collimator, and secondary collimator). Each beam channel in the central collimator's body consists of a primary collimator 65 mm thick from an alloy containing 96 % tungsten and a secondary collimator 92.5 mm thick from lead. The capsule is shown in Fig. 1(b). It is made of stainless steel (SS) and contains 20 cylindrical pellets of 1 mm diameter and 1 mm height with ^{60}Co material. As seen in Fig. 1(c), the capsule is housed within an aluminum bushing system. The distance from the center of the cylindrical cobalt source to the focal point is 401 mm.

The LGK allows the use of four different types of secondary collimators and is made of tungsten with a thickness of 60 mm. The inner and outer collimator diameters of the secondary collimators are given in Table 1 and has been taken from the research of Moskvin et al. [6]. Model B and Model C of LGK both have 201 Cobalt-60 sources arranged on a hemispherical surface with a radius of approximately 420 mm. They are distributed along five latitudes, separated by a 7.5 degree angle [7], corresponding to 5 different source groups denoted from A-E (as shown in Fig. 2). Details of the spherical coordinates of the 201 sources can be found in the research of Banaee et al. [8]. It is not easy to create a structure with 201 sources at once in simulated input. Therefore, we used the geometry and source transform to generate 201 different instances of single-channel source geometries. The distribution of the 201 sources is shown in Fig. 2.

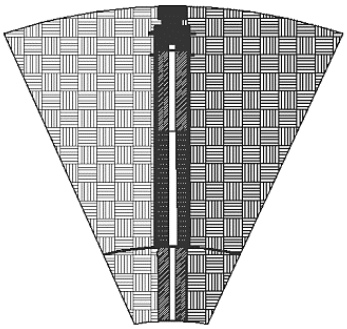

(a)

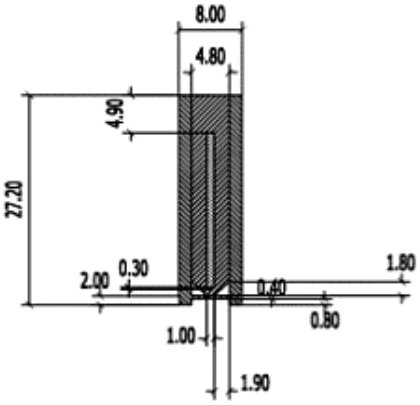

(b)

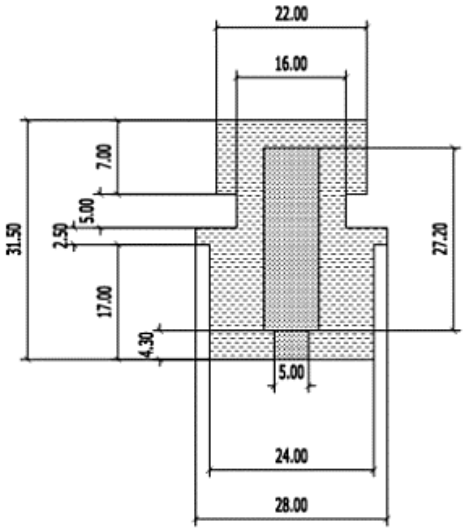

(c)

Fig. 1. Schematic view of the geometrical models used in the simulation for the different parts of LGK. (a) Entire collimator system for a single source. (b) Capsule involving the radionuclide; (c) Bushing system surrounding the capsule.

Table 1. Diameters of the secondary collimators.

Collimator size (mm)	4	8	14	18
Inner radius (mm)	1.00	1.90	3.15	4.15
Outer radius (mm)	1.25	2.50	4.25	5.30

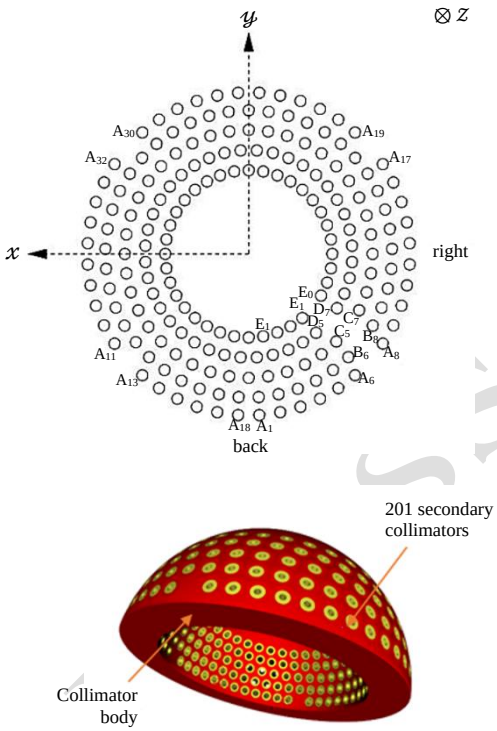

Fig. 2. The modeled collimator body shown in PHIG3D.

With the introduction of the first generation of computers and the Monte Carlo simulation approach, it became feasible to calculate the dose of internal organs. These computational phantoms are extremely comprehensive, providing information on the human body's internal and exterior properties such as shape, density, body volume, and composition. During the 1980s, due to the advent of personal computers and the ability to visualize medical anatomical images in 3D, computational phantoms became popular and widely used. There were three generations of computational phantoms: (a) the stylized phantom, (b) the voxel phantom, and (c) the mesh phantom. They do, however, excel in diverse areas, with mesh-type phantoms outperforming voxel equivalents in terms of flexibility and accurate portrayal of precise patient or subject-specific anatomy [9]. A mesh phantom can be easily modified and calculated more efficiently than a voxel phantom. Therefore, this research employed an adult mesh-type reference phantom from the ICRP-145 publication. The adult mesh-type reference phantom has 163 cm of height and 60 kg of weight constructed by 8.6 million tetrahedrons. A fake spherical tumor with a radius of 15 mm was produced in the center of the adult mesh-type reference phantom's brain, type ICRPAF [10]. Following that, the *.object file was converted into a *.note and *.element file for PHITS and Geant4 using the POLY2TET application. Figure 3 illustrates the adult mesh-type reference phantom integrated into the Geant4 simulation.

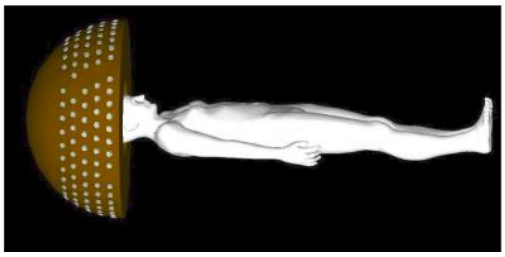

Fig. 3. The adult mesh-type reference phantom with the collimator system demonstrated in Geant4.

The source, as indicated above, can be represented by a cylinder in this simulation. The photons generated by the source have energies of 1.173 MeV and 1.332 MeV with a weight of 1:1 and are emitted in a 3-degree cone opening to shorten simulation time because photons emitted in other directions do not contribute to the region of interest [5]. The total number of histories/events employed in this simulation was 2×10^9, to give a standard error of less than 5 % at the maximal dose region. Electron and photon cutoff energies were chosen at 0.521 MeV and 0.01 MeV, respectively. Similarly to PHITS, the parameters in Geant4 input were set up to be the same as the problem in PHITS.

The investigation was carried out in two stages: (1) dose calculation in an 8-cm spherical water phantom with the interest cube divided into 0.5 mm × 0.5 mm × 0.5 mm scoring bins; and (2) dose calculation in an adult mesh-type reference phantom. The [T-deposit] section was utilized to calculate the deposited dose at each grid bin (sphere phantom case) or organ (adult mesh-type reference phantom case). The result was in the form of Gy/source, which could be converted to a relative dose. The simulations were run on a computer with two Xeon E5 2678 V3 CPUs running at 2.5 GHz using PHITS version 3.24.

RESULTS AND DISCUSSION

Dose calculation in a spherical water phantom

In the case of a single source simulation, Fig. 4 illustrates dose profiles of a collimator 18 mm along the X and Y axes. These results are also compared to Geant4 simulation results using various other physics libraries. StandardPhysics option 3, Livermore, and Penelope are "standard" Geant4 electromagnetic physics libraries, but PHITS employs the same EGS5 algorithm as the EGSnrc simulation code. It can be shown that the PHITS and Geant4 results are in good agreement. In comparison to the other two libraries, the dose curve of the Standard Physics option 3 library is the most similar to the PHITS results. The information in this library is more precise than in the others. It is suitable for medical applications that necessitate a high level of accuracy. However, it takes a long time to simulate.

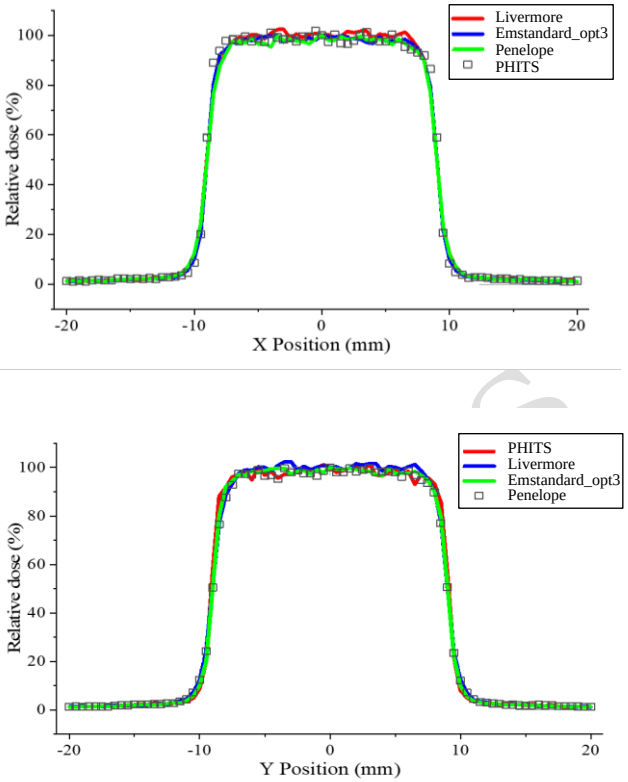

Fig. 4. Comparison of PHITS and Geant4 results for 18-mm collimator.

The PHITS results of the single-channel dose profiles for different collimator sizes (represented by the symbol with a black square) are shown in Fig. 5. These results are also compared with data from Elekta (shown by the green line) and other results from the Monte Carlo method by Cheung et al. [11] (shown by the red line) and Al-Dweri et al. [5] (shown by the blue line). The FWHM and penumbra sizes are shown in Table 2. The FWHM is defined as the radius of the 50 % isodose line, while the penumbra is defined as the distance between the 20 % and 80 % isodose lines. These findings are consistent with results from previous research. The little variations could be attributed to different simulated geometries, the Monte Carlo algorithm, or statistical error. Despite using the same simulation geometry as in Al-Dweri's study, the computational results with PHITS were closer to Elekta's value than in Al-Dweri's study with the PENELOPE code [5]. Furthermore, in the low dose range (outside of the irradiation zone), the dose predicted by PHITS was more accurate than Cheung's results [11]. Even if the dose is mostly caused by a small number of scattered photons, the statistical error remains significant, which can be reduced by increasing the number of histories or utilizing error reduction techniques. The FWHM values are similar to the Al-Dweri's results, but they are very different from the Tian's results. This is not surprising, since Tian's work used a simpler shape [12].

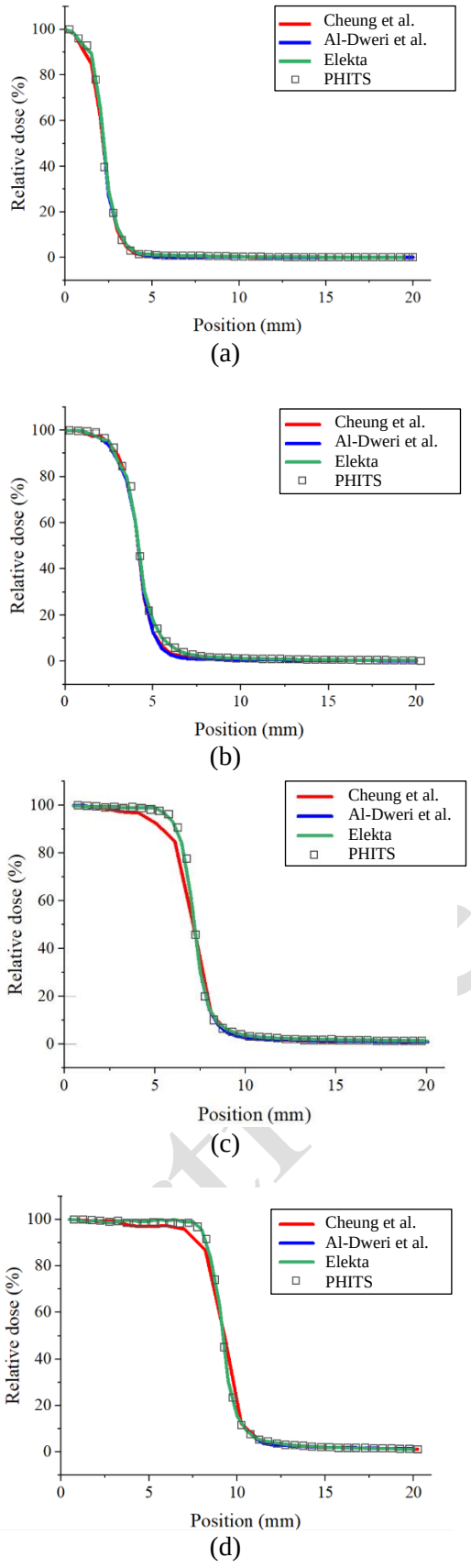

Fig. 5. The dose profile (relative to its maximum) as a function of distance from the center axis for various collimator sizes: (a) 4 mm; (b) 8 mm; (c) 14 mm; and (d) 18 mm.

Table 2. FWHM (50 % of maximum dose) and penumbra (between 80 % and 20 % of maximum dose) values for various collimator helmets compared to other works.

Collimator size (mm)	**18**	**14**	**8**	**4**	**18**	**14**	**8**	**4**
	FWHM (mm)				**Penumbra (mm)**			
PHITS	9.2	7.1	4.2	2.0	1.3	1.4	1.5	1.1
Geant4 (G4EmStandardPhysics option3)	9.1	7.3	4.3	2.1	1.3	1.3	1.4	1.1
Geant4 (G4EmLivermorePhysics)	9.1	-	-	-	1.3	-	-	-
Geant4 (G4EmPenelopePhysics)	9.1	-	-	-	1.3	-	-	-
Al-Dweri et al. (2004)	9.1	7.2	4.2	2.0	1.3	1.4	1.4	1.1
Yuan Tian et al. (2016)	-	-	-	-	1.3	1.2	1.1	1.0

Figure 6 shows the absorbed dose distribution on the three primary planes of the 18 mm collimator when using a narrower simulation grid. It demonstrates that the collimated beams intersect at the center of the spherical phantom as expected. Results of the dose profiles along the X and Z axes of four types of collimators in the case of using full static sources are shown in Fig. 7. It can be seen that the dose profiles along the X or Y will have a penumbra that is greater than that of the Z axis or single source situation. The primary reason for this is an increase in scattered radiation in the X and Y directions because there are differences in the structure of the collimator body along the X or Y axis versus the Z axis.

All simulation results are compared with the treatment planning system Leksell Gamma Plan (LGP), which was used in the study of Trnka et al. [13]. There is good agreement between simulated results and plans. Simulated results are analogous to experimental measurement results. To compare the calculated results and the simulated results, the Gamma Index method was used, as proposed by Low et al. [14]. It evaluates the difference between the calculated and measured dose distributions relative to the acceptance tolerances. A gamma-index distribution can be generated and shown, offering a quantitative assessment of the calculation's quality in regions that meet and fail the acceptance requirements. In this work, this method shows the best collation between simulated results and the planned calculation with 96 %-98 % of the pass rate for criteria of 3 % and three voxels for all collimators.

The output factor is a critical quantity in determining the beam quality produced by the Leksell Gamma Knife device. It is defined as the dose obtained at the focal point of each field divided by the reference field of 18 mm [13].

Table 3 shows the output factor value from the simulation and compares it with other studies. All results from PHITS and Geant4 have the best agreement with Elekta data when compared with other ones. The FWHM and penumbra sizes are shown in Table 4. This means that the simulation of the Leksell Gamma Knife 4C succeeded and that it was able to predict several characteristics correctly.

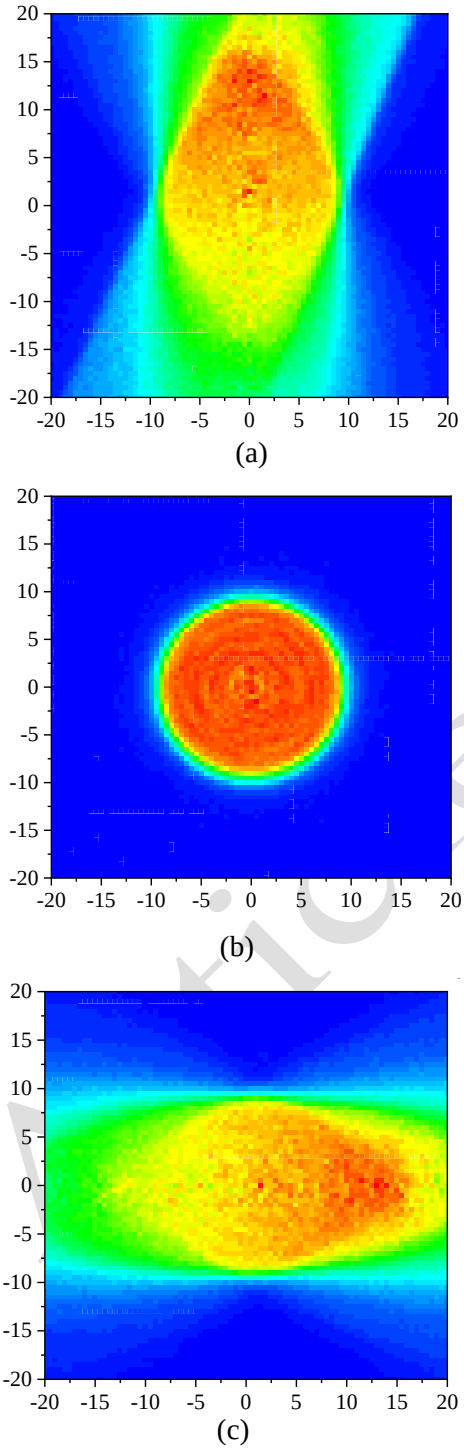

Fig. 6. The color dose map planes for the 18 mm collimator helmet for (A) OXY plane; (b) OYZ plane; and (c) OXZ plane.

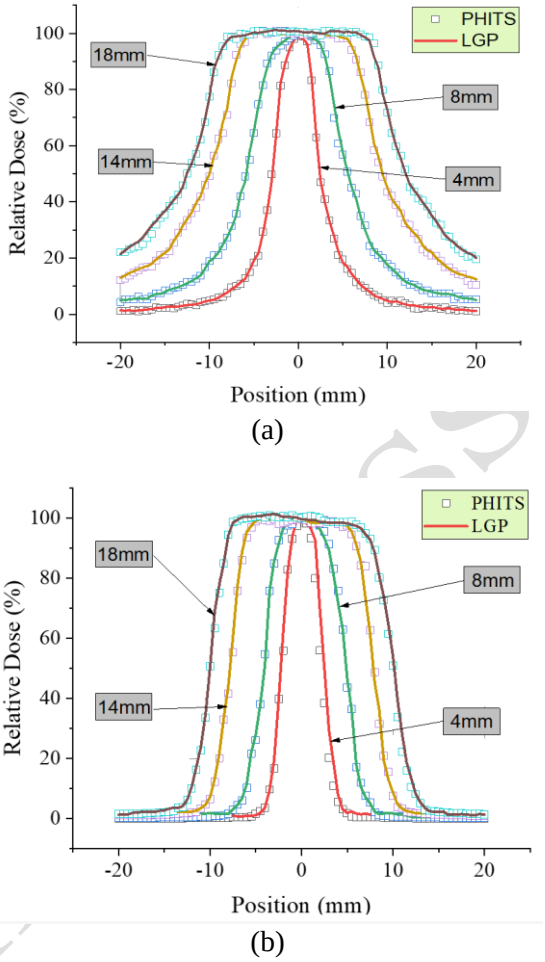

Fig. 7. Relative dose profiles for four types of collimators along the (a) X axis and (b) Z axis.

Table 3. The ouput factor.

Collimator size (mm)	18	14	8	4
PHITS	1.000	0.984	0.949	0.872
Tian et al. [12]	1.000	0.986	0.961	0.880
Moskvin et al. [6]	1.000	0.970	0.946	0.876
Elekta	1.000	0.984	0.956	0.870

Table 4. Comparison of FWHM and penumbra for various collimators (*The values were calculated by the average of the left and right penumbra of each profile). The results were compared with the results in [1].

	FWHM (mm)				Penumbra (mm)*			
Collimator size (mm)	PHITS		Asgari et al.		PHITS		Asgari et al.	
	X	Z	X	Z	X	Z	X	Z
4	5.3	4.5	6.1	4.8	2.6	1.4	2.8	1.3
8	11.4	8.9	11.3	9.1	5.5	2.1	5.0	2.0
14	19.3	15.7	19.4	15.7	8.4	2.1	8.1	2.2
18	24.2	20.0	24.4	20.0	10.3	2.5	10.1	2.4

Dose for a brain tumor and other organs

The above calculation results are completely consistent with previous experimental and simulation studies. This demonstrates that the simulation model of the LGK system is reasonably accurate for carrying out dose calculations for the adult mesh-type reference phantom. In this study, the absorbed dose in the fake tumor was calculated using five distinct source groups (A-E) at the five different collimator body latitudes shown in Fig. 2. As shown in Fig. 8, the highest absorbed dose was used as the reference dose for all cases. It can be seen that the dose differences between the source groups are small. This is due to the fact that the majority of the gamma radiation enters the tumor and is entirely absorbed by it. The relative doses for the 14 mm, 8 mm, and 4 mm collimators were roughly 0.65, 0.25, and 0.05, respectively, when compared to the 18 mm size collimator. The brain structure, which is distinctive among human organ, and the scattering of gamma rays make the contribution to the absorbed dose more complex.

Figure 9 shows that doses in other important organs are much lower than those in the tumor and brain because the beams are collimated into a very small shape. Most of the absorbed doses in other organs far from the tumor are mainly caused by scattered radiation. As a result, they are smaller than absorbed doses in the tumor and the brain, which itself receives just 5 % of the dose received by the tumor. According to Ma et al. [15], the absorbed dose in a single treatment was approximately 40 Gy. Using the above ratio, we can evaluate the absorbed dose for other organs and compare it to what was found in the study [16, 17]. It indicates that the doses in other organs are safe.

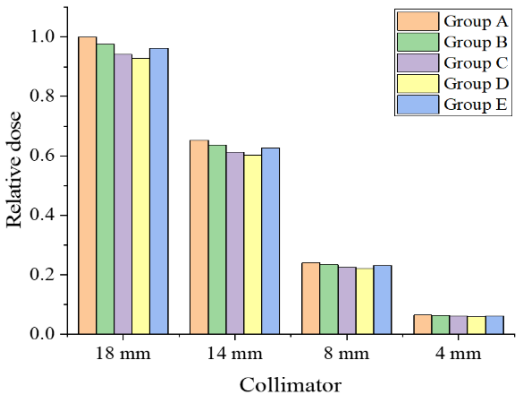

Fig. 8. Comparison of absorbed doses in the turmor from five different source groups (A-E).

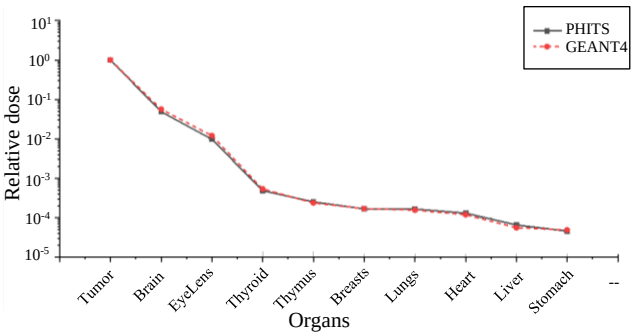

Fig. 9. Relative absorbed doses in other important organs of body.

CONCLUSION

The PHITS code package was employed to simulate the Leksell Gamma Knife system and was compared with other studies. Our calculation of the dose profile, output factor, FWHM, and penumbra shows good agreement with other investigations. Furthermore, this work used simulations with a mesh phantom to calculate absorbed doses in a tumor and other important organs of the body. The PHITS simulation results once again confirmed that radiosurgery of tumors with LGK causes the absorbed doses on other healthy organs of the body to be insignificant and under a safe threshold. With the advantage of being easy to use, supporting users with many new features, and handling complex geometric structures such as tetrahedral mesh, the PHITS code package proved to be very convenient for dose calculation with a mesh-type reference phantom, suitable for simulating the LGK system in this work. The coupled electron/positron and photon transport simulation algorithm agrees well with popular simulation codes such as Geant4.

ACKNOWLEDGMENT

The work presented in this paper has been funded by the Vietnamese Ministry of Education and Training, grant number B2020-BKA-20. The authors would also like to thank the High-performance computing system of the Vietnam Atomic Energy Institute.

AUTHOR CONTRIBUTION

The first author, Hung Bui Tien, and the second author, Duong Tran Thuy, equally contributed as the main contributors of this paper. All authors read and approved the final version of the paper.

REFERENCES

1. S. Asgari, N. Banaee and H. Nedaie, J. Cancer Res. Ther. **14** (2018) 260.
2. J. Y. C. Cheung and K. N. Yu, Med. Phys. **33** (2006) 2500.
3. K. M. Yang, S. J. Madsen, W. L. Chen *et al*., J. Radiosurg. SBRT **1** (2011) 183.
4. A. Wu, G. Lindner, A. H. Maitz *et al*., Int. J. Radiat. Oncol. Biol. Phys. **18** (1990) 941.
5. F. M. O. Al-Dweri, A. M. Lallena and M. Vilches, Phys. Med. Biol. **49** (2004) 2687.
6. V. Moskvin, C. DesRosiers, L. Papiez *et al*., Phys. Med. Biol. **47** (2002) 1995.
7. W. Xiong, D. Huang, L. Lee *et al*., J. Phys. Conf. Ser. **74** (2007) 021023.
8. N. Banaee, S. Asgari and H. Nedaie, Appl. Radiat. Isot. **137** (2018) 154.
9. L. M. Carter, T. M., Crawford, T. Sato *et al*., J. Nucl. Med. **60** (2019) 1802.
10. C. H. Kim, Y. S. Yeom, N. Petoussi-HenssICRP *et al*., Ann. ICRP **49** (2020) 13.
11. J. Y. C. Cheung, K. N. Yu, C. P. Yu *et al*., Med. Phys. **25** (1998) 1673.
12. Y. Tian, H. Wang, Y. Xu *et al*., Biomed. Phys. Eng. Express **2** (2016) 045014.
13. J. Trnka, J. Novotny Jr. and J. Kluson, Med. Phys. **34** (2007) 63.
14. D. A. Low, W. B. Harms, S. Mutic *et al*., Med. Phys. **25** (1998) 656.
15. L. Ma, D. Larson, P. Petti *et al*., Stereotact. Funct. Neurosurg. **85** (2007) 259.
16. B. Emami, J. Lyman, A. Brown *et al*., Int. J. Radiat. Oncol. Biol. Phys. **21** (1991) 109.
17. P. A. Pontoh, O. A. Firmansyah, A. R. Setiadi *et al*., J. Phys. Conf. Ser. **1528** (2020) 012014.
18. J. Allison, K. Amako, J. Apostolakis *et al*., Nucl. Instrum. Methods Phys. Res., Sect. A **835** (2016) 186.